Cellular Signalling 117 (2024) 111094

Contents lists available at ScienceDirect

Cellular Signalling

journal homepage: www.elsevier.com/locate/cellsig

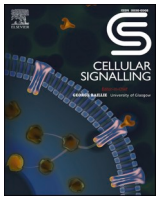

Hypoxia-inducible PRMT2 addiction in glioblastomas

Feng Dong [a,b,1], Xiaoyu Sun [b,1], Jiacheng Su [b], Qian Li [b], You He [b], Wei Li [c], Baofeng Wang [d], Bo Wang [e], Guogang Xu [f,**], Xudong Wu [a,b,g,2,*]

[a] State Key Laboratory of Experimental Hematology, The Province and Ministry Co-sponsored Collaborative Innovation Center for Medical Epigenetics, Key Laboratory of Immune Microenvironment and Disease (Ministry of Education), Tianjin Key Laboratory of Medical Epigenetics, School of Biomedical Engineering & Technology, Tianjin Medical University, Tianjin 300070, China
[b] Department of Cell Biology, Tianjin Medical University, Qixiangtai Road 22, Tianjin 300070, China
[c] Department of Pathology, Tianjin First Central Hospital, Tianjin 300192, China
[d] Department of Neurosurgery, Tongji Hospital, Tongji Medical College, Huazhong University of Science and Technology, Wuhan 430000, China
[e] Department of Neurosurgery, Tianjin Huanhu Hospital, Tianjin Key Laboratory of Cerebral Vascular and Neurodegenerative diseases, Tianjin Neurosurgical Institute, No. 6 Jizhao Road, Tianjin 300350, China
[f] Health Management Institute, The Second Medical Center, Chinese PLA General Hospital, 28 Fuxing Road, Beijing 100853, China
[g] Department of Neurosurgery, Tianjin Medical University General Hospital and Laboratory of Neuro-Oncology, Tianjin Neurological Institute, Tianjin 300052, China

ARTICLE INFO

Keywords:
Hypoxia
Protein arginine methyltransferase 2
Histone arginine methylation
Transcription
Glioblastoma

ABSTRACT

Hypoxia-inducible transcription factors (HIFs) are key transcription factors for cellular response to low oxygen levels. However, the specific mediators responsible for activating downstream transcription are not well characterized. We previously identified Protein Arginine methyltransferase 2 (PRMT2), a highly expressed methyltransferase in glioblastoma multiforme, as a transcription co-activator. And we established a connection between PRMT2-mediated histone H3R8 asymmetric methylation (H3R8me2a) and transcription activation. Here we find that PRMT2 is activated by HIF1α under hypoxic conditions. And we demonstrate that PRMT2 and its H3R8me2a activity are required for the transcription activation of a significant subset of hypoxia-induced genes. Consequently, the inactivation of PRMT2 suppresses hypoxia-induced glioblastoma cell migration, attenuates tumor progression, and enhances chemotherapeutic sensitivity in mouse xenograft models. In addition, our analysis of clinical glioma specimens reveals a correlation between PRMT2 protein levels, HIF1α abundance, and an unfavorable prognosis. Our study establishes HIF1α-induced PRMT2 as a critical modulator in the activation of hypoxia-related transcriptional programs, ultimately driving malignant progression.

1. Introduction

During tumor progression, a hypoxic niche is formed as the tumor outgrows its existing blood and oxygen supply capacity. In response to low oxygen levels, tumor cells produce various factors, such as vascular endothelial growth factor (VEGF), to promote the formation of new blood vessels through angiogenesis. However, the resulting tumor vasculature is often structurally abnormal and functionally compromised, further perpetuating hypoxia. In addition to angiogenesis, other adaptive responses arise under hypoxic conditions, such as metabolic reprogramming and alterations in the tumor microenvironment. These adaptions contribute to genetic instability, enhancing proliferative and metastatic potential, and resistance to therapies [1–3]. Glioblastoma (GBM) is one of the most malignant brain tumors and is highly resistant to anti-VEGF therapies [4–7]. Gaining a molecular understanding of the formation and pathological effects of the hypoxic niche is crucial in the development of targeted therapies aimed at combating GBM progression.

In response to hypoxia, a crucial regulatory factor for the activated transcriptional program is the hypoxia-inducible factor (HIF), which

* Corresponding author at: State Key Laboratory of Experimental Hematology, The Province and Ministry Co-sponsored Collaborative Innovation Center for Medical Epigenetics, Key Laboratory of Immune Microenvironment and Disease (Ministry of Education), Tianjin Key Laboratory of Medical Epigenetics, Department of Cell Biology, Tianjin Medical University, Qixiangtai Road 22, Tianjin 300070, China.
** Corresponding author.
E-mail addresses: gxu@301hospital.org (G. Xu), wuxudong@tmu.edcu.cn (X. Wu).
[1] These authors contributed equally.
[2] Lead contact.

https://doi.org/10.1016/j.cellsig.2024.111094
Received 7 January 2024; Received in revised form 1 February 2024; Accepted 7 February 2024
Available online 8 February 2024

consists of a family of heterodimeric transcription factors (TFs) composed of α and β subunits. Under normal oxygen conditions (normoxia), the two main isoforms of HIF-α (HIF1α and HIF2α) undergo prolyl hydroxylation by prolyl hydroxylase enzymes (PHDs), leading to their degradation. Under normoxia condition, prolyl hydroxlate domain proteins (PHDs) which needs oxygen as subunit hydroxylates HIFs at the proline residues (Pro 402 and Pro 564) in the HIF ODDD. Meanwhile, factor inhibiting HIF1 (FIH1) hydroxylates asparagine on HIF1α C-TAD domain, resulting in HIF1α binding with von hippel-lindau (VHL) and inhibition of interacting with co-factor P300/CBP, and then E3 ligase recognizes and binds to VHL leading to proteasome degradation [8]. However, in hypoxic conditions, the activity of PHDs is inhibited, resulting in the stabilization and nuclear translocation of HIF-α [9,10], enabling the activation of gene transcription.

Although the post-translational regulation of HIF-α is well understood, the mechanisms underlying its interactions with chromatin regulators and the activation of target genes remain poorly understood. Apart from potential nucleosome remodeling functions of HIF1α itself [11], several histone modifiers have been identified to act as co-factors for transcription regulation [12–15]. In our previous study, we identified Protein Arginine methyltransferase 2 (PRMT2) as a transcriptional co-activator, catalyzing asymmetric dimethylation on histone H3R8 (H3R8me2a). Furthermore, we found that PRMT2 is highly expressed in GBM and is essential for tumor progression [16]. However, the adaptation of PRMT2 expression and activity to complex microenvironments, such as hypoxic niches, and its impact on potential pro-tumorigenic transcriptional programs during tumor progression, remains largely unknown.

In this study, we investigate the potential correlation between PRMT2 and the transcriptional signature associated with hypoxia. Our results unequivocally establish that PRMT2 is transcriptionally activated by HIF1α, providing strong evidence for its involvement in hypoxia-induced gene regulation. We further demonstrate that PRMT2 plays a critical role in the transcriptional activation of a specific subset of genes that are responsive to hypoxia, and this activity is dependent on its H3R8me2a activity. Most importantly, we highlight the indispensable role of PRMT2 activity in driving tumor progression under hypoxic conditions. Therefore, our study expands our understanding of the intricate network of transcriptional regulation in response to hypoxia. Moreover, we identify PRMT2 as a potential target for anti-hypoxia therapeutics in the context of malignant diseases. These findings have promising implications for the development of novel strategies to effectively combat hypoxia-related diseases and improve patient outcomes.

2. Materials and methods

2.1. Tumor samples, animal and study approval

Surgical samples were obtained from patients undergoing resection for newly diagnosed GBMs at the Department of Neurosurgery, Wuhan Tongji Hospital. Written informed consent was received from all participants. This study was approved by the institutional review board of Tongji Hospital and performed in accordance with the Declaration of Helsinki (serial noTJ-1BR20181111). All animal experiments were performed according to Health guidelines of Tianjin Medical University Institutional Animal Use and Care Committee (TMUaMEC-2,017,009).

2.2. Cloning and plasmid preparation

Human HIF1α cDNA was amplified and cloned into pCDH-CMV-MCS-EF1-puro by ClonExpress II One Step Cloning Kit (Vazyme C112) and verified by sequencing. The HIF1α-P402A/P564A/N803A mutation was generated with PCR site-directed mutagenesis (Vazyme P515) and collated by sequencing. Specific oligonucleotides were synthesized (GENEWIZ) and cloned into pLKO.1 TRC cloning vector following the protocol recommended by Addgene. The sequences for primers or oligos are listed in Supplementary Table S1.

2.3. Cell culture

The human glioblastoma cell line U87, Human Embryonic Kidney 293 T, hepatoma carcinoma cell Huh7 and colorectal cancer HCT116 were authenticated as described [17]. U87, 293 T and Huh7 were grown in cultured in Dulbecco's modified Eagle's medium (DMEM) containing 10% fetal bovine serum (FBS) and HCT116 in McCoy's 5 A with 10% FBS. Tumor progenitor cell (TPC) lines TPC1115 was in DMEM/F12 medium supplemented with N2, B27, 20 ng/ml human fibroblast growth factor-basic, 20 ng/ml epidermal growth factor-basic [16]. All cells were maintained at 37 °C with 5% CO2, but hypoxia experiments were conducted in hypoxic incubator (COY Laboratory Products O2 Control In Vitro Glove Box) with 1% O2. All cells were regularly tested for mycoplasma free.

2.4. PRMT2H112Q cell line construction

Dox-induced PRMT2 expression was achieved using the tetracycline inducible expression system. PRMT2 cDNA was cloned into pLVX-Tight-Puro plasmid by the ClonExpress II One Step Cloning Kit (Vazyme C112) and collated by sequencing. The PRMT2–H112Q mutation was generated with PCR site-directed mutagenesis involved in *Dpn*I enzyme digestion, transformation and sequencing. pLVX-Tight-Puro-PRMT2-H112Q plasmid and rTTA-G418 plasmid was virus-packaged by lentiviral packaging system, and then the two virus are used to co-infect U87 cell. When the mutant protein needs to be expressed, DOX treatment is added in advance.

2.5. Chromatin immunoprecipitation and reverse transcriptionquantitative PCR (ChIP/RT-qPCR)

Chromatin preparation was performed as described [18]. Briefly, cells were cross-linked with 1% formaldehyde for 10 minutes (min) at room temperature (RT) and quenched with 0.125 M glycine for 5 mins. Then, cells were washed, resuspended, lysed, and sonicated with 30 s ultra-sonication at 30 s intervals using a BioRuptor sonicator (Diagenode, Liege, Belgium). The harvested chromatin was incubated overnight at 4 °C with primary antibodies. Anti-HIF1α were purchased from GeneTex (GTX127309). After reverse cross-linking, ChIP DNA was purified using PCR purification kits (QIAGEN, Hilden, Germany) for qPCR analysis.

Total RNA was isolated using TRIGene Reagent (Genstar P118) and subjected to reverse transcription with StarScript III All-in-one RT Mix with gDNA Remover (Genstar A230–10). The RT-qPCR primer sequences are summarized in Supplementary Table S1.

2.6. Immunofluorescence (IF)

Cultured cells were fixed with 4% formaldehyde, permeabilized with 0.1% Triton X-100 in PBS, blocked with 5 mg/ml BSA and incubated overnight with relevant primary antibodies followed by FITC or TRITC-secondary antibody (ZSBIO, dilution 1:200) for 1 h (h) at RT and Hoechst for nuclei staining. The antibodies include anti-HIF1α (1:100; GeneTex, GTX127309), anti-PRMT2 (1:100; LSBio, LS-C482512) and anti-H3R8me2a (1:500; Novus Biologicals, nb21–1062).

2.7. IHC staining

For the IHC staining, specimen slides were deparaffinized, rehydrated, antigen retrieval, blocked and incubated with appropriate primary antibodies. The antibodies included anti-VEGFα (1:100; Absin, abs136982), anti-HIF1α (1:100; GeneTex, GTX127309) and anti-PRMT2 (1:100; LSBio, LS-C482512) and anti-H3R8me2a (1:500; Novus

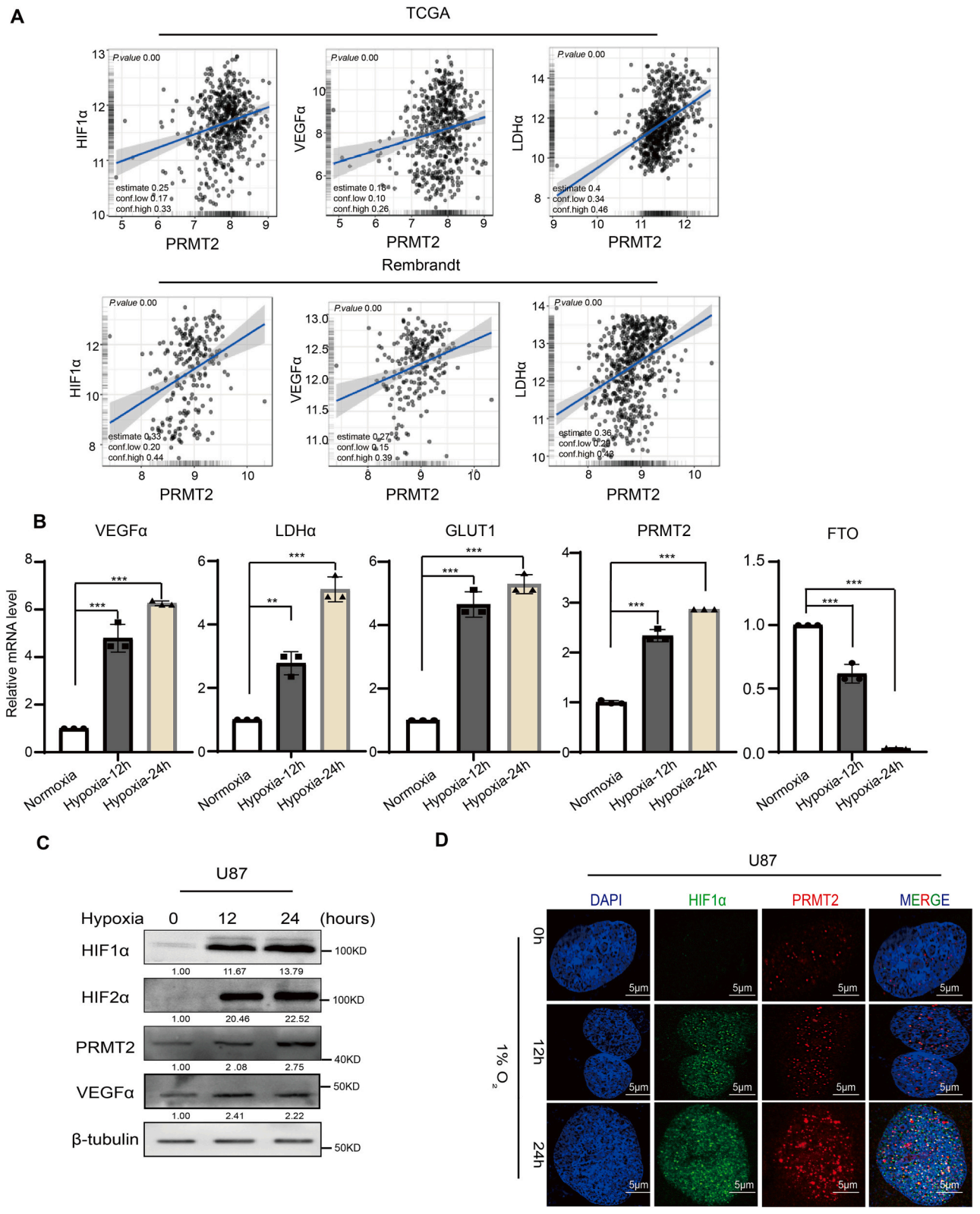

Fig. 1. PRMT2 expression is induced by hypoxia.

(A) Correlation between the mRNA levels of PRMT2, HIFα, VEGFα and LDHα in the TCGA and Rembrabdt RNA-seq dataset. Pearson's product-moment correlation, two.sided.

(B) Hypoxia-induced upegulation of PRMT2, VEGFα, LDHα and GLUT1 expression in U87 were detected by RT-qPCR analysis. White represents normoxia, dark gray represents 12 h hypoxia and light gray represents 24 h hypoxia. FTO downregulation serves as a negative control. Two-tailed unpaired student's *t*-test, $^{**}P < 0.01$, $^{***}P < 0.001$, $n = 3$.

(C) The differential expression of designated proteins in normoxic or hypoxic conditions was determined by WB analysis. β-tubulin serves as a loading control.

(D) Representative IF images of U87 cells with PRMT2 and HIF1α antibodies in normoxic or hypoxic conditions. Scale bar, 5 μm.

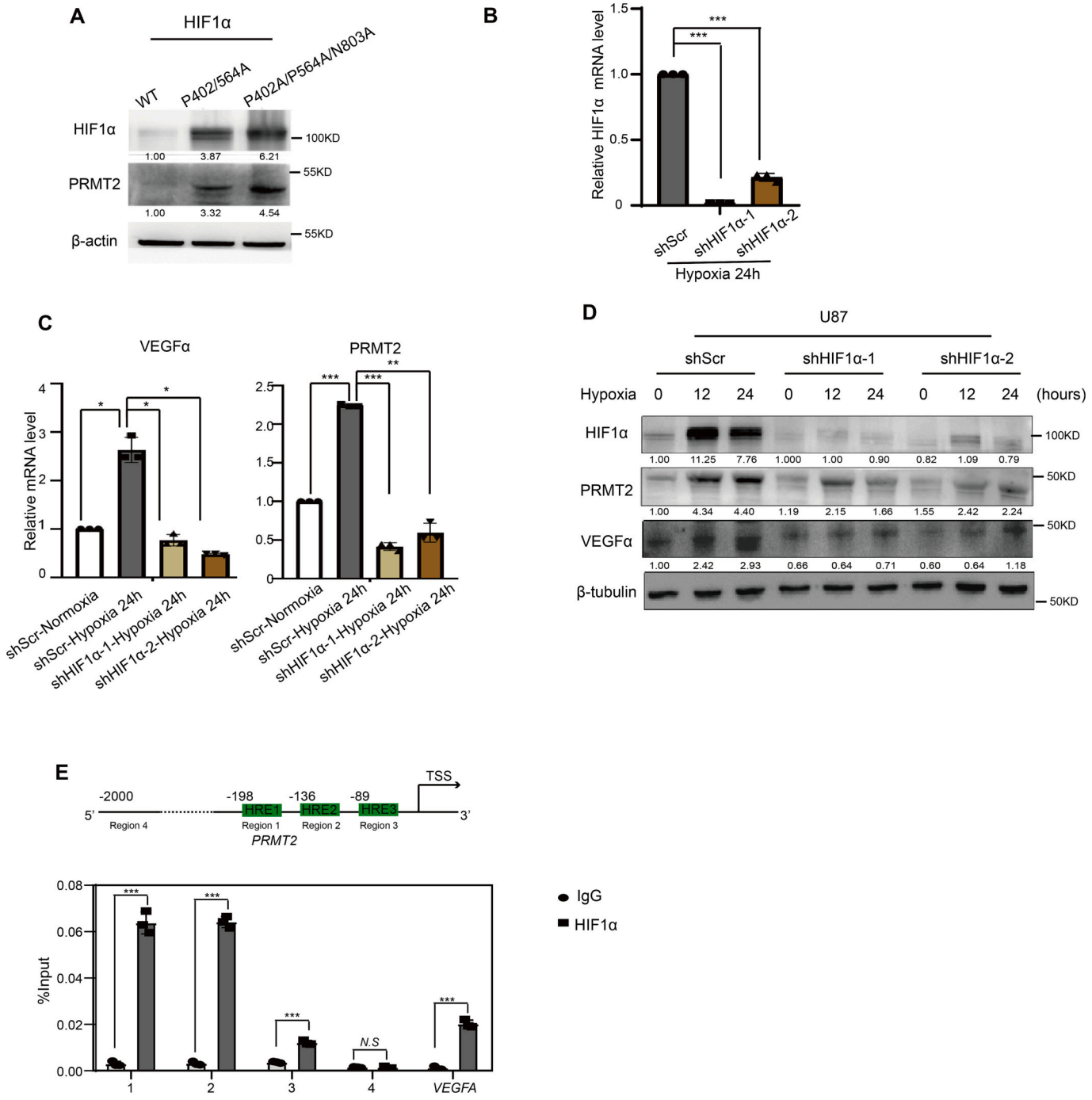

Fig. 2. PRMT2 expression is induced by HIF.

(A) The expression of PRMT2 and HIF1α in U87-HIF1α-WT or mutant cells were determined by WB analysis. β-actin serves as a loading control.

(B-D) The expression levels of HIF1α (B), PRMT2 and VEGFα (C) in U87 cells transduced with two different shRNA constructs targeting HIF1α (shHIF1α-1 and shHIF1α-2) or scramble shRNA (shScr) were determined by RT-qPCR analysis and and WB analysis (D). White represents shScr in normoxia, dark gray represents shScr with 24 h hypoxia, light brown represents shHI1Fα-1 with 24 h hypoxia and dark brown represents shHI1Fα-2 with 24 h hypoxia. Two-tailed unpaired student's t-test, $^{***}P < 0.001$, n = 3. β-tubulin serves as a loading control for WB analysis.

(E) ChIP-qPCR assay testing the HIF1α enrichment at the hypoxia response element (HRE) of *PRMT2* and *VEGFα* in U87 cultured under hypoxia. Above: Schematic of the promoter of *PRMT2* and *VEGFα*. Green-marked box indicates the location of hypoxia response elements (HRE). Two-tailed unpaired student's *t*-test, $^{***}P < 0.001$, n = 3. (For interpretation of the references to colour in this figure legend, the reader is referred to the web version of this article.)

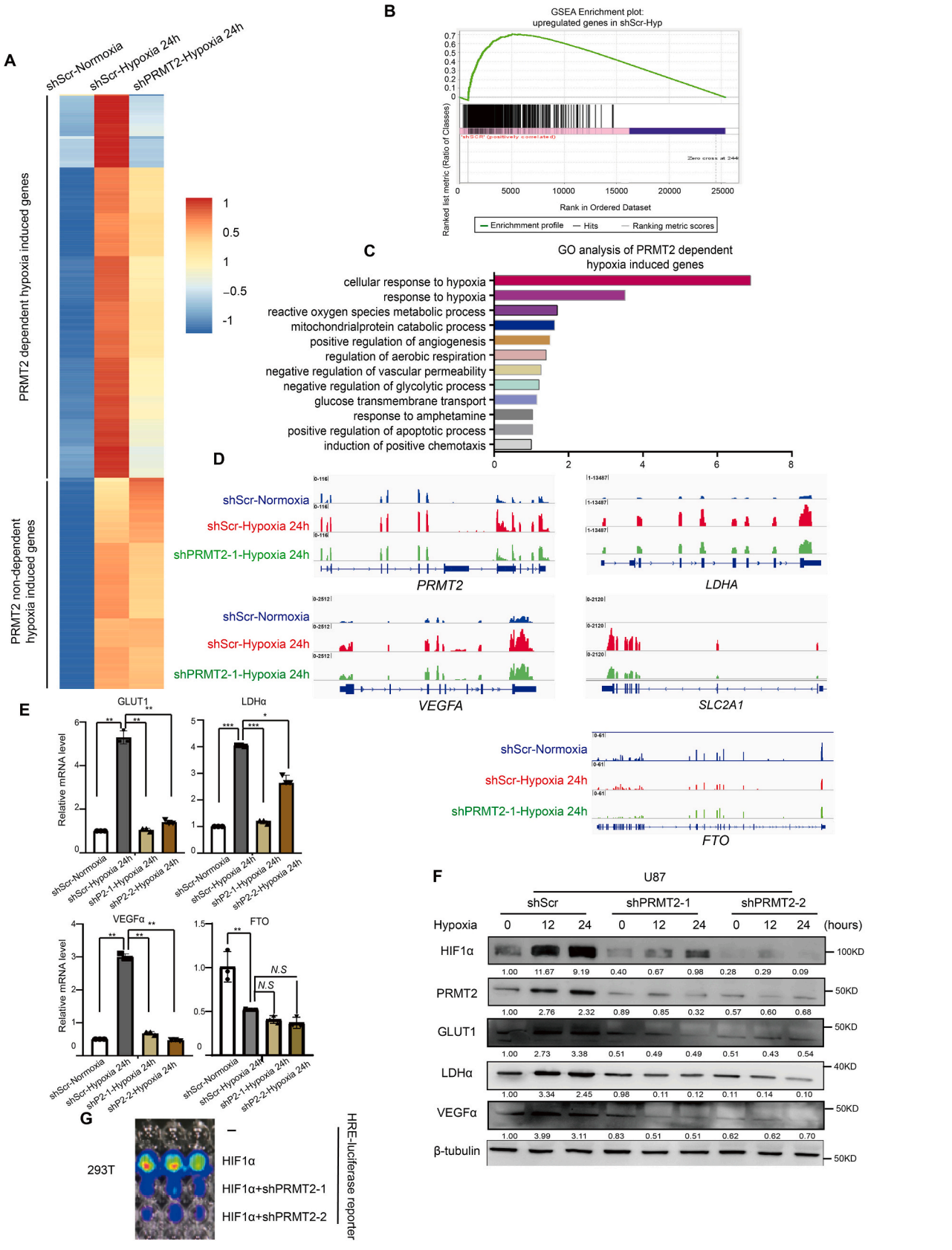

(caption on next page)

Fig. 3. PRMT2 plays active roles in the transcription response to hypoxia.
(A) Heatmap show the hypoxia induced genes in U87 shScr and shPRMT2 cells with or without hypoxia. Filtered by log2 (fold change) ≥1 and false discovery rate (FDR) < 0.05.
(B) GSEA indicates upregulated hypoxia-induced genes (456 genes, $P < 0.001$) is significantly enriched in the control group (shScr-Hyp), compared with PRMT2-depleted group (shPRMT2-Hyp).
(C) GO analysis of PRMT2-dependent hypoxia-induced genes. Tops of enrichment of each biological process are shown.
(D) Genomic snapshots of RNA-seq analyses of representative genes in designated groups of cells.
(E and F) The expression level of GLUT1, LDHα, VEGFα and FTO in the corresponding U87 cells were detected by RT-qPCR (E) and WB analysis (F). White represents shScr in normoxia, dark gray represents shScr with 24 h hypoxia, light brown represents shPRMT2–1 with 24 h hypoxia and dark brown represents shPRMT2–2 with 24 h hypoxia. Two-tailed unpaired student's *t*-test, $^{*}P < 0.05$, $^{**}P < 0.01$, $^{***}P < 0.001$, n = 3. β-tubulin serves as a loading control for WB analysis.
(G) HRE-Luciferase-reporter assay was employed to confirm the effect of PRMT2 on luciferase expression in designated groups of 293 T cells ($1*10^4$). (For interpretation of the references to colour in this figure legend, the reader is referred to the web version of this article.)

Biologicals, nb21–1062). According to the percentage of positive cells and staining intensity, the statistics analysis for the IHC staining were scored: 1 if 0–25% of the tumor cells showed positive staining, 2 if 26–50% of cells were stained, 3 if 51–75% stained, and 4 if 76–100% stained.

2.8. Tumor size measurement

Female BALB/C nude mice (6 weeks old) were used in all tumor experiments and transplanted into the frontal lobes of brains. The BALB/C nude mice bearing U87 iPRMT2-H112Q cells (4×10^5) were fed with water containing 0.2% doxycycline and (or) injected with 10 mg/kg TMZ. Bioluminescence xenogen imaging (IVIS SPECTRUM, PE) was used to monitor tumor growth. Luciferin (15 mg/ml in DPBS) was prepared and injection amount was determined by 10 μ/g of body weight.

2.9. Western blot (WB)

To obtain whole-cell protein extracts, cells were harvested and lyzed as previously described. The corresponding primary antibodies used for immunoblotting included anti-HIF1α (1:1000; GeneTex, GTX127309, RRID:AB_2616089), anti-HIF2α (1:1000; Abclonal, A7553, RRID: AB_2768078), anti-β-tubulin (1:10000; Abclonal, AC021, RRID: AB_2773004), anti-PRMT2 (1:1000; LSBio, LS-C482512) and anti-H3R8me2a (1:1000; Novus Biologicals, nb21–1062). And Direct-load Colour Prestained Protein Marker (M221, GenStar) was used in all WB assays.

2.10. HRE-luciferase-reporter assay

Plasmid pCDH-CMV-MCS-EF1-HIF1A (P402A/P564A/N803A) was transfected into 293 T HRE-luciferase reporter cells with or without shPRMT2. Two days later, a certain number of cells were placed in 96-well plates and 1 μl Luciferin (15 mg/ml) was added in cell medium for 10 min. Instrument IVIS SPECTRUM (PE) is used to detect cell bioluminescence.

2.11. RNA-sequencing (RNA-seq) analysis

For RNA-seq, library construction, sequencing, and data analysis were performed at Novogene. Log_2 (FPKM+1) values were used to generate heatmap with scaling in the row direction.

2.12. CUT&Tag

The CUT&Tag assay was performed as described previously [18]. In brief, 10,000–50,000 cells were harvested and washed twice in 1 ml wash buffer (20 mM HEPES *pH* 7.5, 150 mM NaCl, 0.5 mM Spermidine, Protease Inhibitor Cocktail (PIC, Bimake). Concanavalin A coated beads were activated by washing twice in binding buffer (20 mM HEPES *pH* 7.5, 10 mM KCl, 1 mM $MnCl_2$, 1 mM $CaCl_2$). Then activated beads and resuspended cells were incubated for 0.5 h at RT. After primary antibody was incubated, the beads were resuspended in 100 ml Dig wash buffer (20 mM HEPES *pH* 7.5, 150 mM NaCl, 0.5 mM Spermidine, 0.0125% Digitonin, PIC) containing 1 ml Guinea Pig anti-Rabbit IgG antibody. After being washed three times, 0.04 mM pA-Tn5 adapter complex (Vazyme S603) was added and incubated for 1 h at RT. Beads were incubated in 300 ml tagmentation buffer (20 mM HEPES *pH* 7.5, 300 mM NaCl, 0.5 mM Spermidine, 0.0125% Digitonin, 10 mM $MgCl_2$, PIC) for 1 h at 37 °C, followed by stopping tagmentation and DNA extraction. The purified DNA was amplified and corresponding fragments were recovered for sequencing. The constructed libraries were sequenced with PE150 on NovaSeq platform.

2.13. Statistics

Statistics were performed using Prism software GraphPad Prism 8. A two-tailed unpaired student's *t*-test and Pearson's correlation test were used as appropriate. *P* value of <0.05 was supposed statistically significant.

3. Results

3.1. PRMT2 expression is upregulated in response to hypoxia

To gain insights into the adaptability of PRMT2 in the hypoxic microenvironment, we utilized TCGA and Rembrabdt datasets of adult GBM. Through our analysis, we discovered a positive correlation between the expression levels of PRMT2 and the levels of HIF1α, VEGFα and LDHα (Fig. 1A). To establish a direct correlation, we subjected U87, a GBM cell line, to hypoxic conditions. Using RT-qPCR analyses, we observed that the elevation of PRMT2 expression does not occur immediately, in contrast to the rapid and continuous upregulation of well-known hypoxia marker genes such as VEGFα, LDHα, and GLUT1 (Fig. 1B). Furthermore, at the protein level, the increase in PRMT2 expression appears to be secondary to the rapid stabilization of HIF1α and HIF2α (Fig. 1C and D). These findings strongly suggest that PRMT2 expression is likely induced by HIF in response to hypoxia.

3.2. PRMT2 expression is induced by HIF

To provide conclusive evidence that the induction of PRMT2 expression is indeed dependent on HIFs, we employed PHD-resistant HIF1α mutants [19,20]. As depicted in Fig. 2A, these mutations effectively stabilized HIF1α, resulting in a significant upregulation of PRMT2 expression, even under normoxic conditions. Moreover, by successfully silencing HIF1α expression (Fig. 2B) in U87 cells, we observed a failure to induce PRMT2 and VEGFα expression in response to hypoxia (Fig. 2C and D). To further support this finding, we conducted ChIP-qPCR analysis of HIF1α in hypoxia-treated U87 cells, revealing a substantial enrichment of HIF1α at three putative hypoxia response elements (HRE) of *PRMT2* (analyzed by the Eukaryotic Promoter Database), similar to the enrichment at the HRE of *VEGFA* promoter (Fig. 2E). Consequently, it becomes evident that the elevated expression of PRMT2 is directly induced by HIF.

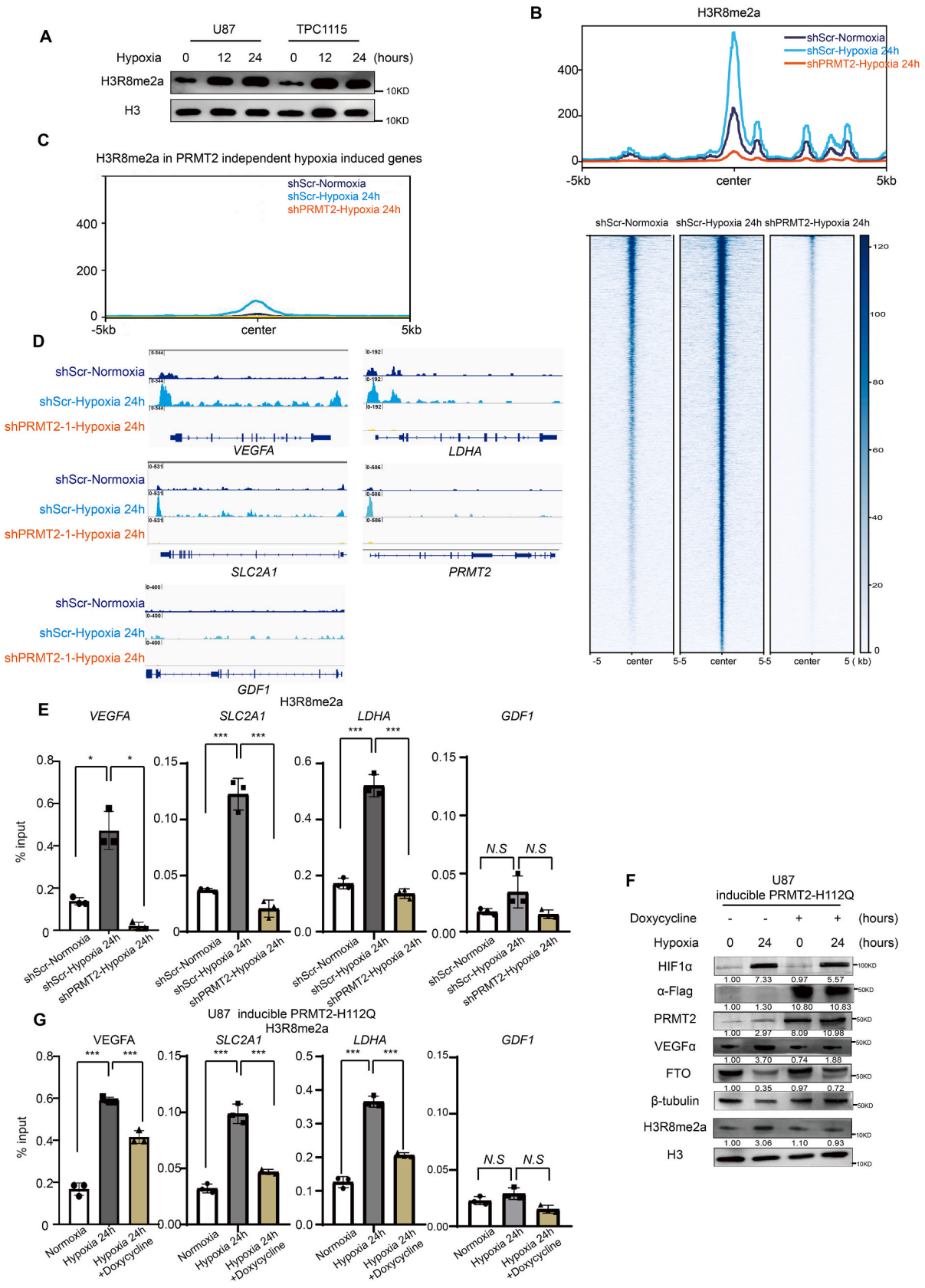

(caption on next page)

Fig. 4. PRMT2 modulates transcription response to hypoxia through its H3R8me2a activity.
(A) WB analysis of H3R8me2a levels in U87 and TPC1115 cells expressing shScr or shPRMT2. Histone 3 was used as loading control.
(B) Average profile and heatmap of H3R8me2a across a genomic window of ±5000 bp surrounding the peak summit in designated groups of U87 cells.
(C) Low or no H3R8me2a signals across a genomic window of ±5000 bp PRMT2-independent hypoxia induced genes in designated groups of U87 cells.
(D) Genomic snapshots of H3R8me2a CUT&Tag analyses of representative genes with positive or negative enrichment of H3R8me2a in designated groups of cells.
(E) ChIP-qPCR analysis of H3R8me2a enrichment on the promoter regions of PRMT2 target genes in PRMT2-depleted cells cultured in normoxic or hypoxic conditions. White represents shScr in normoxia, dark gray represents shScr with 24 h hypoxia and light brown represents shPRMT2 with 24 h hypoxia. The *GDF1* promoter serves as a negative control. Error bars, mean ± SD, n = 3.
(F) Cellular levels of PRMT2, VEGFα HIFα and H3R8me2a in U87 cells with or without PRMT2-H112Q expression. In order to induce PRMT2-H112Q expression, cells were treated with or without Doxycycline (Dox 1 mg/L) for 96 h in normoxic or hypoxic conditions. β-tubulin and H3 serve as a loading control.
(G) ChIP-qPCR analysis of H3R8me2a enrichment on the promoter regions of PRMT2 target genes in PRMT2 mutated cells cultured in normoxic or hypoxic conditions. White represents normoxia, dark gray represents 24 h hypoxia and light brown represents dox treated PRMT2-H112Q with 24 h hypoxia. The *GDF1* promoter serves as a negative control. Error bars, mean ± SD, n = 3. (For interpretation of the references to colour in this figure legend, the reader is referred to the web version of this article.)

3.3. PRMT2 plays active roles in the transcription response to hypoxia

Considering that PRMT2 acts as a transcription co-activator [16], we sought to determine whether the increased expression of PRMT2 is merely a consequence of hypoxia or a key driver of the hypoxia-associated transcriptional program. To verify this, we performed PRMT2 knockdown experiments in U87 cells and subjected them to 24 h of hypoxia exposure. Our RNA-seq analysis revealed that out of the 456 hypoxia-induced genes, 65.1% (297 genes) are dependent on PRMT2 (Fig. 3A). Gene Set Enrichment Analysis (GSEA) demonstrated a significant enrichment of hypoxia-induced genes (HIGs) in the control group compared to PRMT2-depleted cells (Fig. 3B). Furthermore, Gene Ontology (GO) analysis of this subset of genes highlighted a significant enrichment in processes related to hypoxia response and glycolysis (Fig. 3C). The differential expression of three representative HIGs, including *GLUT1*, *LDHα*, and *VEGFα*, between control and PRMT2-depleted cells, is shown in Fig. 3D. As a negative control, FTO expression is not responsive to hypoxia or PRMT2 depletion (Fig. 3D). These effects were further validated through independent examinations using RT-qPCR and WB analyses (Fig. 3E and F). Importantly, we observed similar results in TPC1115 (primary cultured glioblastoma cells) and other cancer cell types (Huh7, HeLa), as depicted in Supplementary Fig. S1A and B. These findings suggest that PRMT2, upon being activated by HIFs, further drives the hypoxia-induced transcriptional regulatory network.

To further confirm the critical role of PRMT2 in downstream effects on HIF1α, we generated an HRE-luciferase reporter. As illustrated in Fig. 3G, overexpression of HIF1α significantly increased luciferase activity, which was attenuated by PRMT2 depletion. Hence, PRMT2 serves as a driver of the transcriptional response to hypoxia rather than merely a passenger.

3.4. PRMT2 modulates transcription response to hypoxia dependent on its H3R8me2a activity

Given the critical of PRMT2 in catalyzing H3R8me2a [16,21], we examined whether hypoxia affects the levels of H3R8me2a. As shown in Fig. 4A, the global levels of H3R8me2a are strikingly increased in response to hypoxia. To determine whether these changes in H3R8me2a are PRMT2-dependent, we performed genome-wide analysis of H3R8me2a using CUT&Tag. Intriguingly, after exposure to hypoxia, control U87 cells exhibited 3938 H3R8me2a peaks, which were significantly downregulated at PRMT2 dependent hypoxia induced genes. In contrast, little or no enrichment of H3R8me2 was observed for the PRMT2-independent hypoxia induced genes (Fig. 4B-C). The enrichment of H3R8me2a on three representative HIGs, including *VEGFα*, *LDHα*, *GLUT1*, and interestingly *PRMT2* itself, is shown in Fig. 4D and independently validated through ChIP-qPCR analysis. The absence of H3R8me2a at the *GDF* loci serves a negative control (Fig. 4D-E). These findings highlight the crucial role of PRMT2-mediated H3R8me2a in the transcriptional response to hypoxia.

To further confirm the effects on H3R8me2a is dependent on the catalytic activity of PRMT2, we generated a Doxycycline (Dox) inducible expression construct of PRMT2H112Q mutant (Fig. 4F). WB analysis revealed that the induction of H3R8me2a and VEGFα levels were moderately affected by this catalytically inactive mutation (Fig. 4F). Moreover, the effects were further supported by the locus-specific enrichment of H3R8me2a on typical HIGs, with the *GDF* loci serving a negative control (Fig. 4G). Collectively, our findings indicate that hypoxia-induced PRMT2 activity results in increased genome-wide H3R8me2a levels, ultimately modulating the expression of HIGs.

3.5. PRMT2 activity is critical for hypoxia-induced cancer cell invasion and self-renewal

To elucidate the impact of increased PRMT2 expression and activity on hypoxia-induced malignancy, we performed transwell assay and a limiting dilution assay for sphere formation using PRMT2-depleted or mutated U87 cells. As shown in Supplementary Fig. S2A-C and Fig. 5A-C, the depletion of PRMT2 in U87 and TPC1115 cells or the induction of the H112Q mutation with Dox had a significant effect on hypoxia-induced cell invasion and self-renewal.

Furthermore, we examined the effect of Desferrioxamine (DFX), a HIF stabilizer, on PRMT2 expression and the cellular phenotype in U87 cells. As expected, DFX strongly induces PRMT2 expression and cell invasion (Fig. S3A). And PRMT2 depletion or inactivation has a significant impact on DFX-induced cell invasion (Fig. S3B-E). These findings underscore the indispensable role of increased PRMT2 activity in hypoxia-induced malignant behavior.

3.6. PRMT2 inactivation prevents chemotherapeutic resistance in vivo

Considering the critical role of cellular response to hypoxia in tumor progression and chemotherapeutic resistance, we aimed to investigate whether inactivation of PRMT2 could enhance the anti-GBM effects of Temozolomide (TMZ). As described previously [16], we established orthotopic mouse models using Dox-inducible PRMT2H112Q-U87 cells transduced with a lentivirus expressing luciferase. The xenografted mice were fed with either Dox-containing or Dox-free water since intracerebral transplantation. Three weeks after transplantation, one of the two groups of mice received two rounds of TMZ treatment, with each round lasting for five days (Fig. 5D). The temporal dynamics of tumor progression and mouse survival were recorded.

As illustrated by the bioluminescence imaging, the tumor volumes appear significantly smaller after Dox induction, for either control (−TMZ) or TMZ-treated (+TMZ) group. Remarkably, the tumors became barely visible after two weeks of combination treatment involving Dox induction and TMZ administration (Fig. 5E and F). Furthermore, Kaplan-Meier survival curves demonstrated a significant extension of survival in the xenografted mice receiving the combination treatment compared to the control (−TMZ) or TMZ monotherapy group (+TMZ; -DOX) (Fig. 5G). Morphological analysis of hematoxylin-eosin-stained brain slides revealed an invasive phenotype in the control group, with tumors infiltrating into the neighboring normal brain tissue. In contrast, no

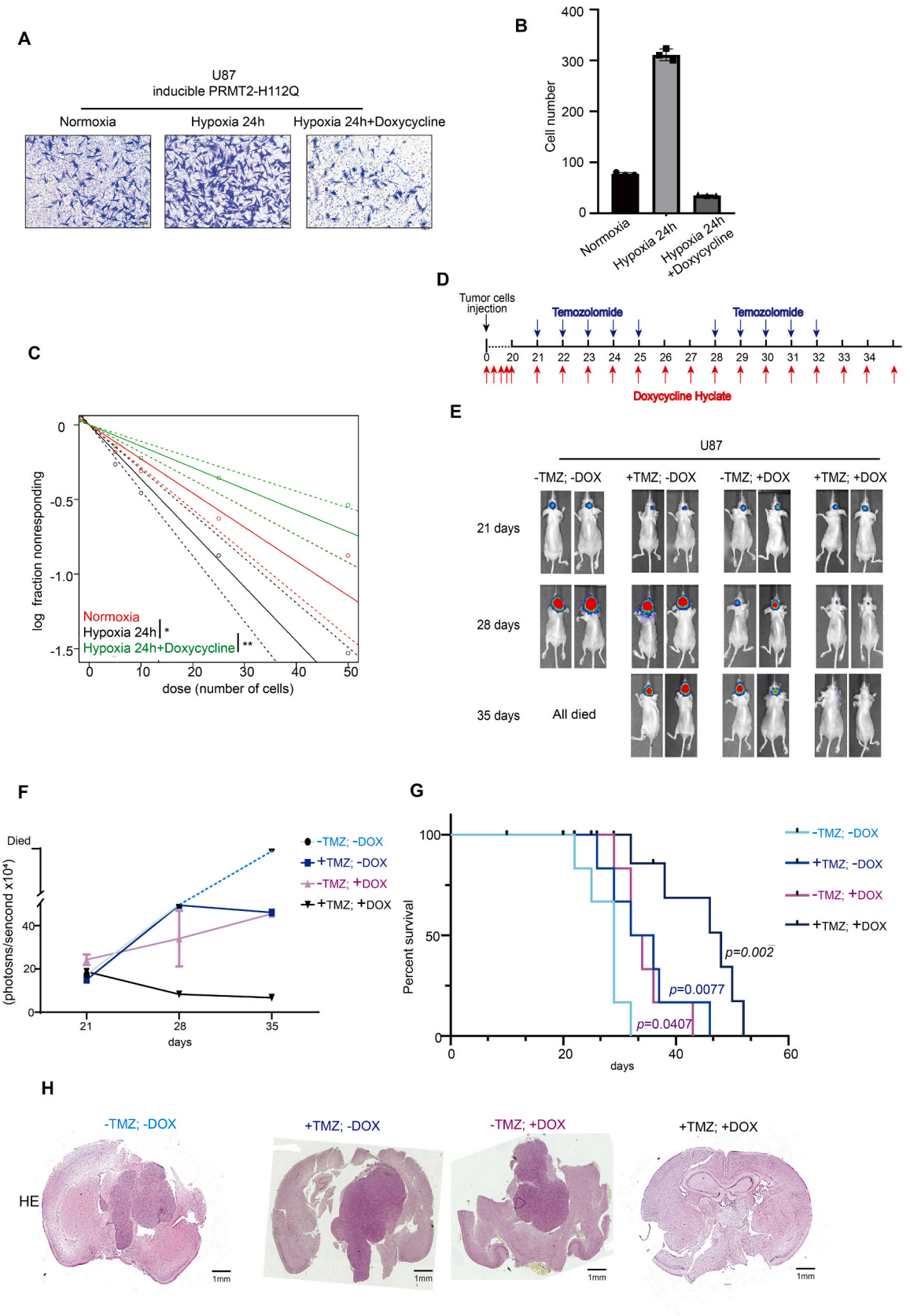

(caption on next page)

Fig. 5. PRMT2 activity is critical for hypoxia-induced cancer cell malignancy and TMZ resistance.
(A and B) Transwell assays were performed to measure the migration ability of U87 inducible PRMT2-H112Q cells in normoxic or hypoxic conditions. Representative examples of crystal violet stainings (A) and statistics analysis (B) are shown. Scale bars, 50 μm. Two-tailed unpaired Student *t*-test, n = 3.
(C) Frequency of sphere-initiating cells as measured by limiting dilution analysis in U87 iPRMT2-H112Q cells cultured in normoxic or hypoxic conditions. Frequency and probability estimates were computed using the ELDA software. $*P < 0.05$, $**P < 0.01$.
(D) Schematic of dosage regimen about Dox induction of PRMT2-H112Q and/or temozolomide (TMZ) treatment.
(E) Representative luciferase images of three mice per group at 21-, 28- and 35-days post tumor implantation. Colour scale for U87 cells: Min = 6.00 × e4, Max = 5.00 × e5.
(F) The average luciferase activity in implanted mice brains at different time points were respectively compared in in designated groups of U87 cells (mean ± SD; n = 6).
(G) Survival analysis of mice intracranially implanted with indicated groups of U87 cells. X axis represents days after cells injection. Significance level was determined using log-rank analysis. n = 6 for each treatment group.
(H) Representative images of H&E staining for tumor formation in the indicated groups. Scale bar, 200 μm. (For interpretation of the references to colour in this figure legend, the reader is referred to the web version of this article.)

apparent tumors were observed in the combination-treated group (Fig. 5H). Therefore, PRMT2 inactivation significantly enhances chemotherapeutic sensitivity in GBM.

3.7. PRMT2 levels and activities are correlated with hypoxia signatures and unfavorable prognosis

To elucidate the clinical significance of the aforementioned observations, we conducted an examination of PRMT2 protein levels and its H3R8me2 activity, along with HIF1α and VEGFα protein levels. Utilizing a glioma tissue array comprising 75 resected human GBM specimens, we discovered a significant correlation between in situ HIF1α and VEGFα protein levels and the intensity of PRMT2 and H3R8me2a staining (Fig. 6A). Based on PRMT2 scoring, we classified the samples into PRMT2-high and PRMT2-low groups. Representative immunohistochemistry (IHC) staining of these groups is depicted in Fig. 6B. Notably, patients with PRMT2-high tumors exhibited markedly shorter survival compared to the PRMT2-low group (Fig. 6C), despite receiving similar surgical and chemical therapies. These findings strongly indicate that PRMT2 levels and activity serve as prognostic indicators for poor outcomes in GBM patients.

4. Discussion

Hypoxia has been tightly linked to several hallmarks of cancers. However, direct targeting of hypoxia signaling still possesses inherent limitations [1,3]. Gaining a profound understanding of the mechanisms through which hypoxia reshapes tumors and their microenvironment, as well as how tumor cells adapt to and flourish in hypoxic conditions, will pave the way for novel approaches in the treatment of hypoxic tumors. In this study, we have demonstrated that PRMT2 functions beyond its role as a downstream target of HIF, serving as a hub that activates hypoxia-inducible genes. These mechanistic insights into the regulatory roles and pro-oncogenic functions of PRMT2 seamlessly integrate into the hypoxic niche.

Actually, PRMT2 was previously identified as one of hypoxia-induced PRMTs in mice [22]. Here we present direct evidence that the expression of PRMT2 is transcriptionally induced by stabilized HIF1. Despite its role as a chromatin regulator, the precise mechanisms underlying HIG activation mechanisms for PRMT2 remain unclear. In contrast to a prior investigation [23], our attempts to observe a physical interaction between HIF1α and PRMT2 were unsuccessful (data not shown). Thus, PRMT2 appears distinct from other transcription cofactors, such as SET1B [13], which is recruited by HIF1 to HREs. Further endeavors aimed at unraveling the molecular basis for PRMT2 binding to chromatin would greatly contribute to deciphering the potential HIF1-independent regulatory mechanism.

Due to unavailability of ChIP-grade antibody, we failed to obtain direct profiling of PRMT2 at the genome wide. Nevertheless, PRMT2 is supposed to be responsible for the regulation of a large subset of target genes through H3R8me2a activity, considering that it is currently the only known enzyme responsible for this modification. Moreover, our RNA-seq analysis shows that PRMT2 dependent HIGs are extensively enriched in response to hypoxia, encompassing processes such as metabolic reprogramming, angiogenesis and vascular abnormality, etc. (Fig. 3C). While the precise mechanisms underlying this selective activation are yet to be fully understood, they may involve local recruitment of PRMT2 or be driven by specific gene promoters. Interestingly, similar to the H3K4me3 methyltransferase MLL1 [24] , HIF1α is also activated by hypoxia-induced PRMT2. These regulatory networks may contribute to a nuanced response to hypoxia.

From the perspective of cancer biology, the identification of PRMT2 as a potential biomarker and its association with patient outcomes highlight the translational implications of our research. Building upon our mechanistic understanding, we have successfully validated the significant role of inhibiting PRMT2 enzyme activity in enhancing the sensitivity of chemotherapy. Therefore, the development of tailored PRMT2 inhibitors becomes imperative. Designing and characterizing specific inhibitors that effectively and selectively target PRMT2's enzymatic activity would not only deepen our understanding of its precise role in tumor progression but also pave the way for the development of personalized treatment strategies for GBM patients.

Funding

This study was supported by the Key Research Project of Tianjin Education Commission (2020ZD13 to X.W.).

CRediT authorship contribution statement

Feng Dong: Writing – original draft, Writing - review & editing, Methodology, Investigation, Data curation, Formal analysis, Conceptualization. **Xiaoyu Sun:** Conceptualization, Methodology, Investigation, Formal analysis, Data curation. **Jiacheng Su:** Investigation, Data curation, Formal analysis. **Qian Li:** Software, Formal analysis, Data curation, Writing - original draft, Writing - review & editing. **You He:** Investigation, Data curation, Formal analysis. **Wei Li:** Investigation, Data curation, Formal analysis. **Baofeng Wang:** Data curation and Formal analysis. **Bo Wang:** Resources. **Guogang Xu:** Writing – original draft, Writing - review & editing, Supervision, Formal analysis. **Xudong Wu:** Writing - original draft, Writing – review & editing, Supervision, Resources, Investigation, Funding acquisition, Conceptualization.

Declaration of competing interest

The authors declare no relevant conflicts of interest.

Data availability

RNA-seq and CUT&Tag data can be downloaded from GEO data repository with accession number GSE235438.

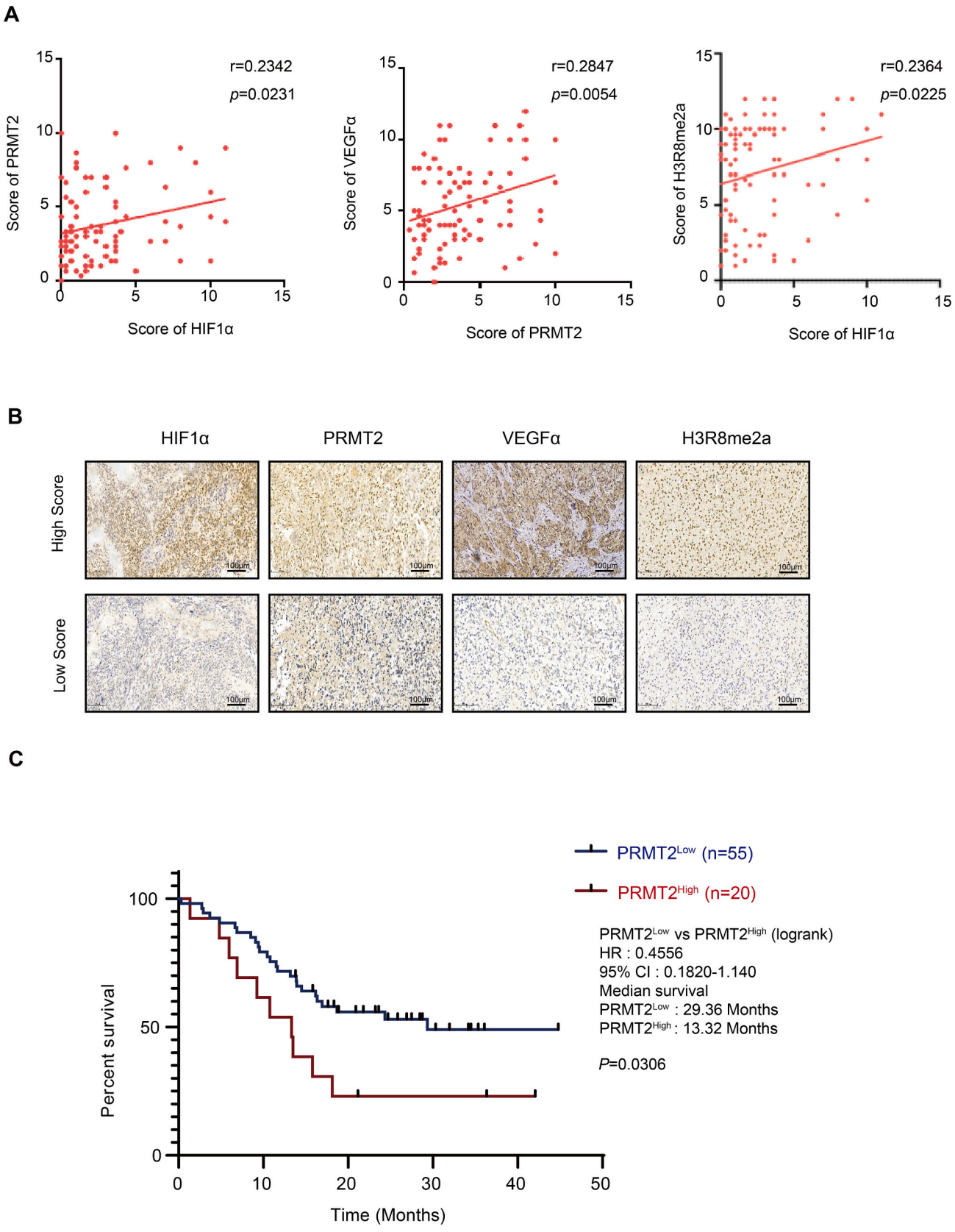

Fig. 6. PRMT2 levels and activities are correlated with hypoxia signatures and unfavorable prognosis.
(A) Correlation of HIF1α and VEGFα with PRMT2 and H3R8me2a protein levels. Significance of the correlation was determined by the Pearson correlation test.
(B) Representative IHC images of PRMT2, VEGFα, H3R8me2a and HIF1α immunostainings. Scale bar, 100 μm.
(C) COX analysis of overall survival in a set of 75 GBM patients with different levels of PRMT2. $P = 0.035$.

Acknowledgments

We thank the Core Facility of Research Center of Basic Medical Sciences, high performance computing (HPC) platform at Tianjin Medical University for technical support. The HRE-Luc construct was a kind gift from Dr. Weilin Jin (LZU).

Appendix A. Supplementary data

Supplementary data to this article can be found online at https://doi.org/10.1016/j.cellsig.2024.111094.

References

[1] G.Z. Qiu, M.Z. Jin, J.X. Dai, W. Sun, J.H. Feng, W.L. Jin, Reprogramming of the tumor in the hypoxic niche: the emerging concept and associated therapeutic strategies, Trends Pharmacol. Sci. 38 (2017) 669–686, https://doi.org/10.1016/j.tips.2017.05.002.

[2] Q. Xiong, B. Liu, M. Ding, J. Zhou, C. Yang, Y. Chen, Hypoxia and cancer related pathology, Cancer Lett. 486 (2020) 1–7, https://doi.org/10.1016/j.canlet.2020.05.002.

[3] Z. Chen, F. Han, Y. Du, H. Shi, W. Zhou, Hypoxic microenvironment in cancer: molecular mechanisms and therapeutic interventions, Signal Transduct. Target. Ther. 8 (2023) 70, https://doi.org/10.1038/s41392-023-01332-8.

[4] K. Szklener, M. Mazurek, M. Wieteska, M. Waclawska, M. Bilski, S. Mandziuk, New directions in the therapy of glioblastoma, Cancers (Basel) 14 (2022), https://doi.org/10.3390/cancers14215377.

[5] C. Lu-Emerson, D.G. Duda, K.E. Emblem, J.W. Taylor, E.R. Gerstner, J.S. Loeffler, T.T. Batchelor, R.K. Jain, Lessons from anti-vascular endothelial growth factor and anti-vascular endothelial growth factor receptor trials in patients with glioblastoma, J. Clin. Oncol. 33 (2015) 1197–1213, https://doi.org/10.1200/JCO.2014.55.9575.

[6] X. Guo, S. Wang, Y. Wang, W. Ma, Anti-PD-1 plus anti-VEGF therapy in multiple intracranial metastases of a hypermutated, IDH wild-type glioblastoma, Neuro-Oncology 23 (2021) 699–701, https://doi.org/10.1093/neuonc/noab005.

[7] Y.C. Lim, K.E. Jensen, D. Aguilar-Morante, L. Vardouli, K. Vitting-Seerup, R. C. Gimple, Q. Wu, H. Pedersen, K.J. Elbaek, I. Gromova, et al., Non-metabolic functions of phosphofructokinase-1 orchestrate tumor cellular invasion and genome maintenance under bevacizumab therapy, Neuro-Oncology 25 (2023) 248–260, https://doi.org/10.1093/neuonc/noac135.

[8] N.S. Kenneth, S. Rocha, Regulation of gene expression by hypoxia, Biochem. J. 414 (2008) 19–29, https://doi.org/10.1042/BJ20081055.

[9] A.J. Majmundar, W.J. Wong, M.C. Simon, Hypoxia-inducible factors and the response to hypoxic stress, Mol. Cell 40 (2010) 294–309, https://doi.org/10.1016/j.molcel.2010.09.022.

[10] E.L. LaGory, A.J. Giaccia, The ever-expanding role of HIF in tumour and stromal biology, Nat. Cell Biol. 18 (2016) 356–365, https://doi.org/10.1038/ncb3330.

[11] N. Suzuki, N. Vojnovic, K.L. Lee, H. Yang, K. Gradin, L. Poellinger, HIF-dependent and reversible nucleosome disassembly in hypoxia-inducible gene promoters, Exp. Cell Res. 366 (2018) 181–191, https://doi.org/10.1016/j.yexcr.2018.03.020.

[12] M.Z. Wu, Y.P. Tsai, M.H. Yang, C.H. Huang, S.Y. Chang, C.C. Chang, S.C. Teng, K. J. Wu, Interplay between HDAC3 and WDR5 is essential for hypoxia-induced epithelial-mesenchymal transition, Mol. Cell 43 (2011) 811–822, https://doi.org/10.1016/j.molcel.2011.07.012.

[13] B.M. Ortmann, N. Burrows, I.T. Lobb, E. Arnaiz, N. Wit, P.S.J. Bailey, L.H. Jordon, O. Lombardi, A. Penalver, J. McCaffrey, et al., The HIF complex recruits the histone methyltransferase SET1B to activate specific hypoxia-inducible genes, Nat. Genet. 53 (2021) 1022–1035, https://doi.org/10.1038/s41588-021-00887-y.

[14] I. Kim, J.W. Park, Hypoxia-driven epigenetic regulation in cancer progression: a focus on histone methylation and its modifying enzymes, Cancer Lett. 489 (2020) 41–49, https://doi.org/10.1016/j.canlet.2020.05.025.

[15] Y. Wang, Y. Lyu, K. Tu, Q. Xu, Y. Yang, S. Salman, N. Le, H. Lu, C. Chen, Y. Zhu, et al., Histone citrullination by PADI4 is required for HIF-dependent transcriptional responses to hypoxia and tumor vascularization, Sci. Adv. 7 (2021), https://doi.org/10.1126/sciadv.abe3771.

[16] F. Dong, Q. Li, C. Yang, D. Huo, X. Wang, C. Ai, Y. Kong, X. Sun, W. Wang, Y. Zhou, et al., PRMT2 links histone H3R8 asymmetric dimethylation to oncogenic activation and tumorigenesis of glioblastoma, Nat. Commun. 9 (2018) 4552, https://doi.org/10.1038/s41467-018-06968-7.

[17] F. Dong, X. Qin, B. Wang, Q. Li, J. Hu, X. Cheng, D. Guo, F. Cheng, C. Fang, Y. Tan, et al., ALKBH5 facilitates hypoxia-induced paraspeckle assembly and IL8 secretion to generate an immunosuppressive tumor microenvironment, Cancer Res. 81 (2021) 5876–5888, https://doi.org/10.1158/0008-5472.CAN-21-1456.

[18] D. Huo, Z. Yu, R. Li, M. Gong, S. Sidoli, X. Lu, Y. Hou, Z. Dai, Y. Kong, G. Liu, et al., CpG island reconfiguration for the establishment and synchronization of polycomb functions upon exit from naive pluripotency, Mol. Cell 82 (2022) 1169–1185, e1167, https://doi.org/10.1016/j.molcel.2022.01.027.

[19] D. Lando, D.J. Peet, D.A. Whelan, J.J. Gorman, M.L. Whitelaw, Asparagine hydroxylation of the HIF transactivation domain a hypoxic switch, Science (New York, N.Y.) 295 (2002) 858–861.

[20] R.K. Bruick, S.L. McKnight, A conserved family of prolyl-4-hydroxylases that modify HIF, Science (New York, N.Y.) 294 (2001) 1337–1340.

[21] S.A. Blythe, S.W. Cha, E. Tadjuidje, J. Heasman, P.S. Klein, beta-catenin primes organizer gene expression by recruiting a histone H3 arginine 8 methyltransferase, Prmt2, Dev. Cell 19 (2010) 220–231, https://doi.org/10.1016/j.devcel.2010.07.007.

[22] A.O. Yildirim, P. Bulau, D. Zakrzewicz, K.E. Kitowska, N. Weissmann, F. Grimminger, R.E. Morty, O. Eickelberg, Increased protein arginine methylation in chronic hypoxia: role of protein arginine methyltransferases, Am. J. Respir. Cell Mol. Biol. 35 (2006) 436–443, https://doi.org/10.1165/rcmb.2006-0097OC.

[23] N.L. Ka, G.Y. Lim, S.S. Kim, S. Hwang, J. Han, Y.H. Lee, M.O. Lee, Type I IFN stimulates IFI16-mediated aromatase expression in adipocytes that promotes E(2)-dependent growth of ER-positive breast cancer, Cell. Mol. Life Sci. 79 (2022) 306, https://doi.org/10.1007/s00018-022-04333-y.

[24] J.M. Heddleston, Q. Wu, M. Rivera, S. Minhas, J.D. Lathia, A.E. Sloan, O. Iliopoulos, A.B. Hjelmeland, J.N. Rich, Hypoxia-induced mixed-lineage leukemia 1 regulates glioma stem cell tumorigenic potential, Cell Death Differ. 19 (2012) 428–439, https://doi.org/10.1038/cdd.2011.109.